nature climate change

Article

https://doi.org/10.1038/s41558-024-01957-9

Historical impacts of grazing on carbon stocks and climate mitigation opportunities

Received: 9 April 2023

Accepted: 19 February 2024

Published online: 15 March 2024

Check for updates

Shuai Ren[1,2,3] ✉, César Terrer[2] ✉, Juan Li[1], Yingfang Cao[4], Shanshan Yang[1] & Dan Liu[1] ✉

Grazing has been associated with contrasting effects on soil carbon stocks at local scales, but accurate global assessments of its net impact are lacking. Here we conducted a meta-analysis of 1,473 soil carbon observations from grazing studies to quantify global changes in soil carbon stocks due to grazing practices. Our analysis shows that grazing has reduced soil carbon stocks at 1-m depth by 46 ± 13 PgC over the past 60 years. The interplay between grazing intensity and environmental factors explains global variations in soil carbon changes. Maps of optimal grazing intensity indicate that implementing grazing management on 21 million km^2 of grazing lands, mainly through decreasing grazing intensity on 75% of lands and increasing it on the rest could result in a potential uptake of 63 ± 18 PgC in vegetation and soils. These results highlight the potential of employing grazing as a climate mitigation strategy.

Soil carbon is an important component of the global carbon cycle, acting as both a source and sink for atmospheric carbon dioxide (CO_2)[1,2], and plays a vital role in climate regulation[3,4]. Globally, the carbon stored in soils is three times larger than in the atmosphere, but its stability is influenced by a range of interrelated factors, including climate[5], soil physical properties[6] and human-induced land use changes such as livestock grazing[7]. Understanding how soil carbon responds to these pressures is key to developing strategies for carbon sequestration and sustainable land management.

Livestock grazing, accounting for 77% of the global farming land[7], plays an important role in the soil carbon cycle[7–10]. Grazing can stimulate plant growth and allocation of carbon to roots and associated microbes, which can lead to an increase in the amount of carbon being taken up from the atmosphere and often stored as mineral-associated organic carbon in the soil[9,11]. However, overgrazing can cause soil erosion and damage to plant inputs, decreasing soil carbon storage[10,12]. Globally, overgrazing has led to extensive land degradation, affecting approximately 262 million hectares[13,14]. Managing grazing in a way that balances the positive and negative impacts on soil carbon stocks is thus crucial.

Understanding the global variations and controls of soil carbon in response to grazing is complex, partly because soil carbon is located belowground and its responses to grazing cannot be detected by satellites[9,12]. Many countries, especially developing countries, have applied the Tier-1 approach from the Intergovernmental Panel on Climate Change (IPCC) for assessing soil carbon changes due to grazing[15]. This approach employs default stock change factors at a depth of 30 cm (ref. 16). While straightforward to implement, the simplified Tier-1 method lacks the granularity needed to capture spatial and depth variations in soil carbon changes due to grazing. Addressing these issues is a critical step to understand the extent to which improved grazing management can serve as an efficient climate strategy for carbon sequestration[17].

In this Article, we used a database of 1,473 paired soil carbon stock observations to assess global patterns of carbon stock changes in different soil layers due to grazing and estimate carbon sequestration potential from grazing optimization at a global scale (Supplementary Fig. 1 and Extended Data Fig. 1). The sign of soil carbon stock changes in response to grazing varies within the database, with declines, remaining unchanged or even increases observed in individual experiments (Supplementary Fig. 2). Therefore, our specific objectives are to (1) use a meta-analysis to quantitatively summarize results across multiple studies, investigate potential predictors of the divergent grazing effects and produce spatially explicit global estimates of grazing-driven

[1]State Key Laboratory of Tibetan Plateau Earth System, Environment and Resources, Institute of Tibetan Plateau Research, Chinese Academy of Sciences, Beijing, China. [2]Department of Civil and Environmental Engineering, Massachusetts Institute of Technology, Cambridge, MA, USA. [3]University of Chinese Academy of Sciences, Beijing, China. [4]Key Laboratory of Cold Regions Restoration Ecology, Northwest Institute of Plateau Biology, Chinese Academy of Sciences, Xining, China. ✉e-mail: shuairen@itpcas.ac.cn; cterrer@mit.edu; liu.dan@itpcas.ac.cn

https://doi.org/10.1038/s41558-024-01957-9

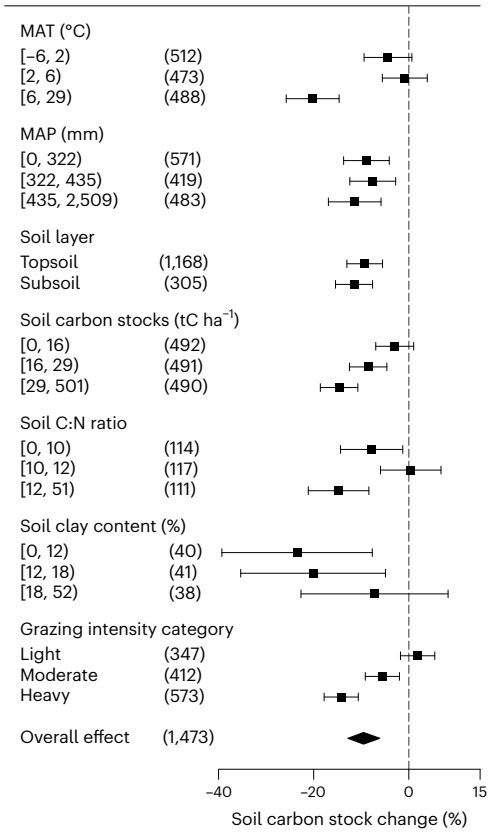

Fig. 1 | Meta-analysis of the grazing effects on soil carbon stocks across different factors. n = 1,473. Overall means and 95% CIs are shown; the grazing effects were considered significant if the 95% CIs did not overlap with zero. Values in parentheses represent sample sizes. See Supplementary Table 1 for more details.

carbon stock changes in topsoil (0–30 cm) and subsoil (30–100 cm) over the past 60 years; (2) establish empirical relationships between carbon stock changes, grazing activities and local environmental conditions for each grazing grid, and generate a global map delineating optimal grazing intensities; and (3) evaluate the maximum carbon sequestration achievable through optimized grazing management, offering a targeted approach to climate mitigation.

Potential predictors of soil carbon change under grazing

Overall, grazing significantly reduced soil carbon stocks by 9.5% across experiments (Fig. 1; 95% confidence interval (CI) −13% to −6%, P < 0.001). This reduction, however, is not uniform; the impacts of grazing exhibit substantial variations across environmental and anthropogenic factors (Fig. 1). Using a random-forest approach (Methods), we find that grazing intensity (GI) and temperature best explain the variations in soil carbon stock changes in response to grazing (Supplementary Fig. 3). The relationship between grazing intensity and soil carbon stock change was non-linear across field experiments (Fig. 2, P < 0.001, n = 780); in general, soil carbon stock increases and then decreases with GI. Such a non-linear response might be closely related to root carbon dynamics. The grazing optimization hypothesis suggests that compensatory plant growth occurs at a light or moderate disturbance level[18,19]. In this case, more plant carbon would be allocated to roots, thus favouring carbon accumulation in the soil[20]; however, this is reversed under heavy grazing (Fig. 2). These mechanisms also help explain why there was an overall reduction in soil carbon loss across experiments (9.5%), as about half of these experiments focused on heavy grazing (Fig. 1). To test the hypothesis, we further analysed the relationship of root carbon change with GI across field observations (Methods) and found a similar response pattern as observed in soils (Supplementary Fig. 4, P < 0.001, n = 738). In contrast, the relationship between temperature and soil carbon stock change was significantly negative (Supplementary Fig. 5a, P < 0.001, n = 1,473), primarily attributed to higher microbial activities under warmer conditions[2,6]. Overall, we found that grazed plots characterized by high grazing intensities and warmer climates tend to exhibit more pronounced negative soil carbon responses, and these relationships are secondarily modulated by soil properties such as soil C:N (an indicator of nitrogen availability) and soil depth (Supplementary Fig. 3). However, the grazing effects did not vary significantly across experimental durations and livestock types (Supplementary Figs. 5–8), indicating their limited utility in predicting soil carbon responses to grazing.

Global effects of grazing on soil carbon stocks

We then applied our predictive model (tenfold cross-validation R^2 = 0.61; Supplementary Fig. 9) to scale up the site-level observations across the globe at a 1-km resolution to quantify changes in topsoil and subsoil carbon stocks due to grazing (Fig. 3). Globally, we estimated that livestock grazing has reduced soil carbon stocks by 17 ± 4% at a depth of 1 m over the past 60 years, which corresponds to an absolute loss of 46 ± 13 PgC across about 24 million km^2 of grazing lands (Supplementary Table 2). The predicted soil carbon loss (−17%) is substantially higher compared to process-based model simulations (−5.8%)[13], probably due to the inadequate representation of critical processes related to overgrazing in existing models, such as species composition changes[21], soil compaction due to trampling[9] and nutrient loss due to erosion[22]. Moreover, while soil carbon was lost throughout the soil profile, we observed an increase in loss with increasing depth (Supplementary Table 2). Specifically, compared to the topsoil (−17.3 ± 2.3 PgC), subsoil contributes to more than 60% (−28.4 ± 8.43 PgC) of the total soil carbon loss (Supplementary Table 2).

In general, overgrazing can reduce carbon content at depth through reduced soil carbon inputs due to limited root growth and increased soil carbon outputs due to erosion[8,11,23] (Supplementary Fig. 10a, P < 0.001). Moreover, topsoils are often more susceptible than subsoils to animal trampling, leading to a significant increase in surface soil bulk density (Supplementary Fig. 10b, P < 0.001). These processes, which are particularly pronounced under high grazing pressures prevailing in most parts of the world over last decades[14], together explain the greater reduction of carbon stock in subsoils than in topsoils (Supplementary Table 2 and Fig. 3). The differences in background soil carbon stocks of layers could also partially explain the carbon loss variations, since subsoils typically store large amounts of carbon[2], and a small percentage change can lead to great carbon loss.

Across ecozones, we found that the negative grazing impacts were greatest in the tropics (−23.4%), followed by subtropical (−16.5%) and temperate zones (−15.2%), and lowest in boreal zone (−8%) (Fig. 4a). Specifically, substantial soil carbon loss due to grazing is most evident in southern Asia (−38%) and in central Africa (−30%) (Fig. 3). In contrast, soil carbon in about 5% of the analysed pixels showed minimal or even positive responses to grazing, mainly in mid- to higher latitudes. These patterns hold true for different soil layers and in both relative and absolute terms (Fig. 4a,b). Throughout the tropics, we estimated that grazing has led to a loss of 9.6 ± 0.96 PgC from topsoil and 13.6 ± 3.04 PgC from subsoil, collectively accounting for 51% of the global carbon loss (Supplementary Table 2).

In contrast to the moderate to low pressure levels in colder regions, grazing disturbance is markedly high in most of the tropics (Supplementary Fig. 11), causing severe damage to plant inputs in these areas (Supplementary Figs. 12 and 13). Moreover, in tropical climates, soil microbial activities are high due to the hot climate and soils often have limited carbon stablization capacity as a result of chemical

https://doi.org/10.1038/s41558-024-01957-9

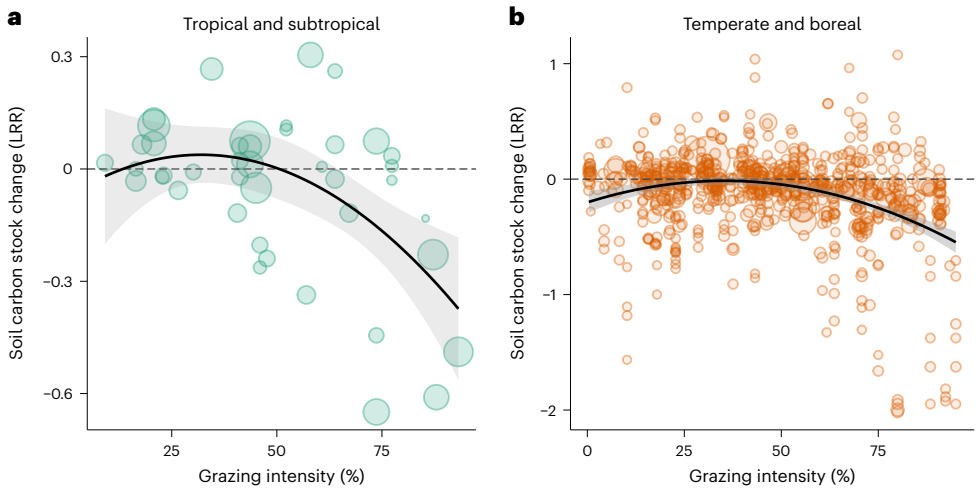

Fig. 2 | Relationships of grazing-driven soil carbon stock changes with grazing intensity. a, Data are from tropical ($n = 24$) and subtropical ($n = 22$) zones. **b**, Data are temperate ($n = 726$) and boreal ($n = 8$) zones. The regression lines in **a** and **b** are based on quadratic meta-regression models ($P < 0.001$; *P* values for two-tailed tests), with 95% CIs (shaded areas). Data shown here are from field grazing experiments, with grazing intensity representing the proportion of aboveground biomass consumed. Dot sizes are proportional to model weights. LRR, log response ratio.

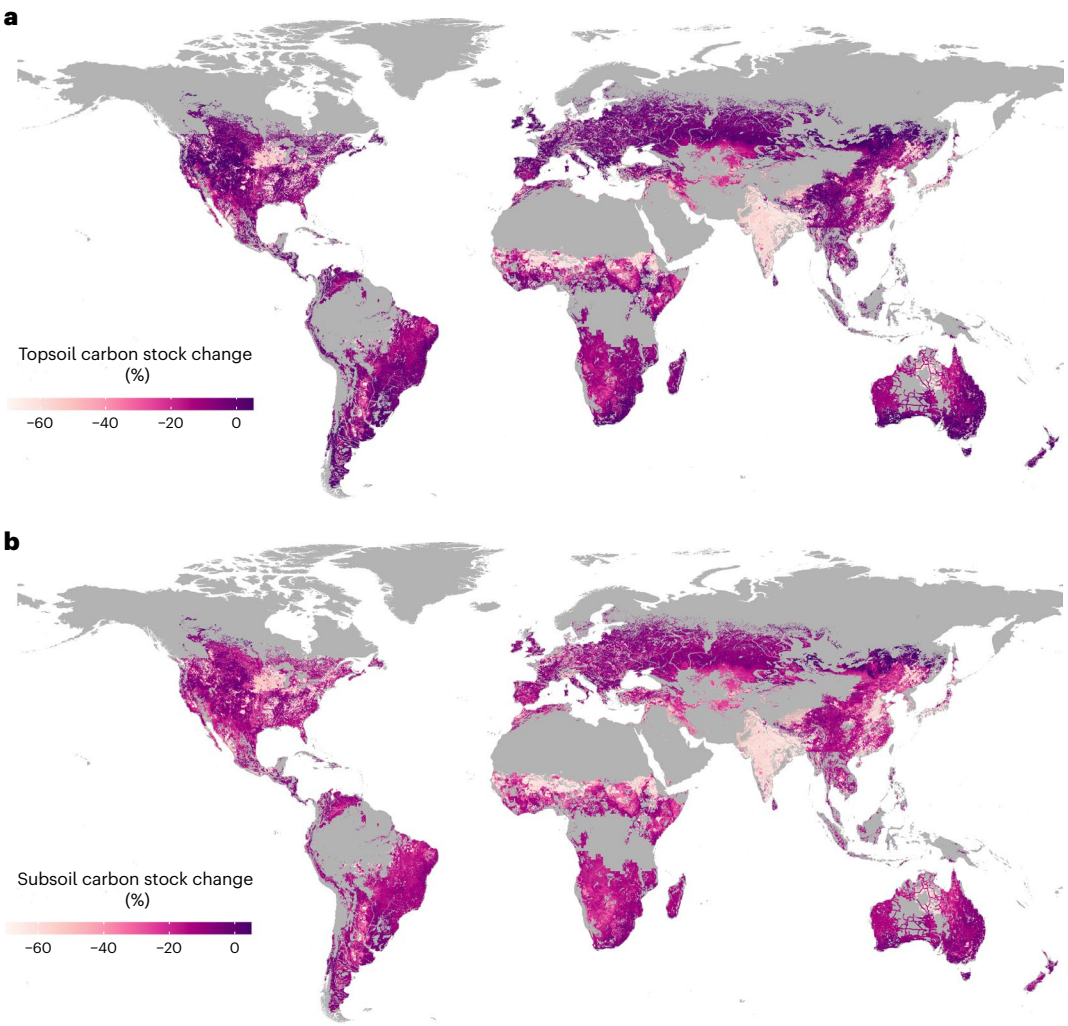

Fig. 3 | Soil carbon stock changes due to livestock grazing. a,**b**, Global grazing-driven soil carbon stock changes (%) for topsoil (0–30 cm; **a**) and subsoil (30–100 cm; **b**) upscaled from grazing experiments.

https://doi.org/10.1038/s41558-024-01957-9

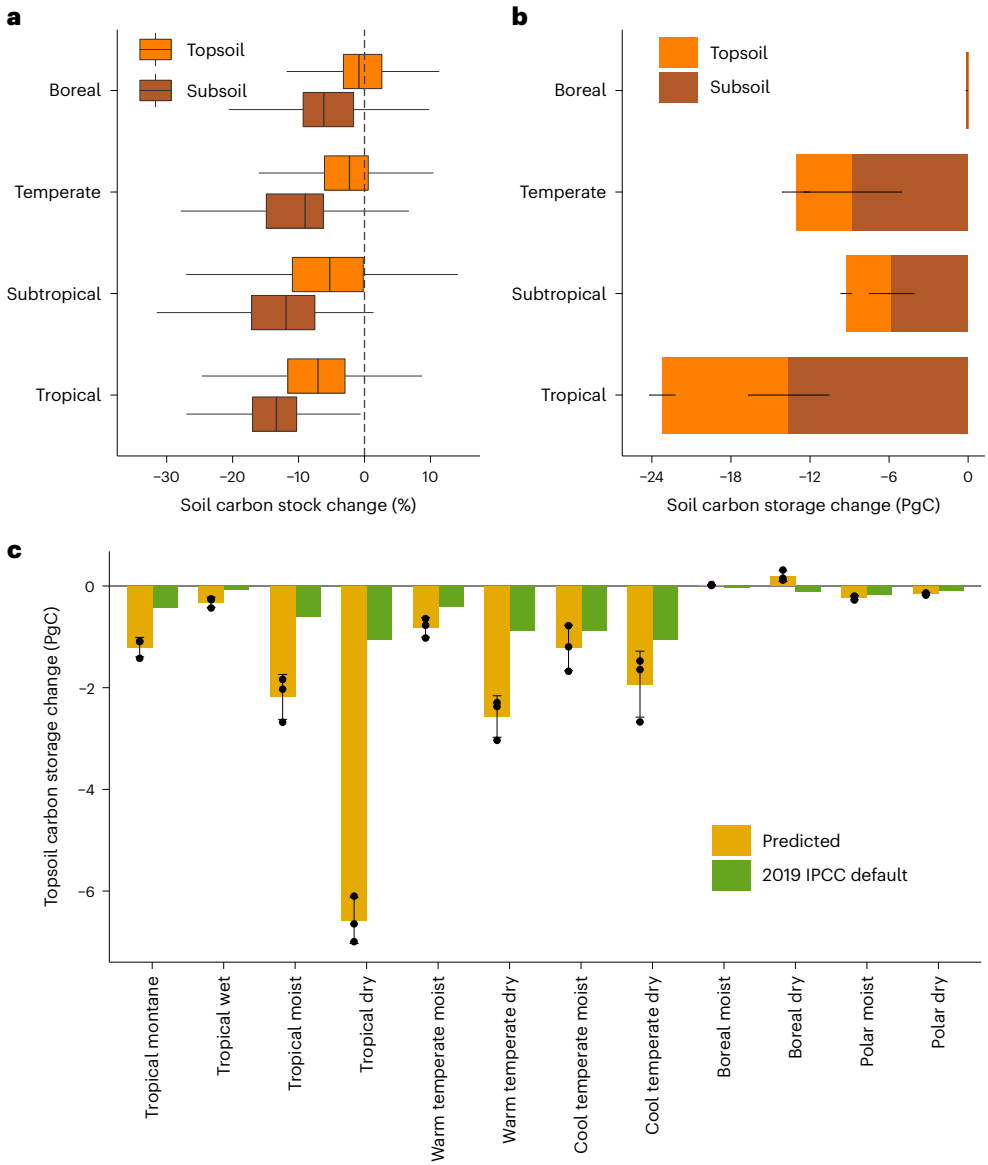

Fig. 4 | Soil carbon changes due to grazing grouped by ecozones. a, Box plot of predicted relative carbon changes (%) per soil layer and ecozone, aggregated from the gridded maps in Fig. 3. **b**, Bar plot represents cumulative partitioned absolute soil carbon changes (PgC) induced by grazing (Methods). **c**, Comparison of predicted topsoil carbon change (PgC) with that calculated using the 2019 IPCC default stock change factors (Methods). Box plot shows the 25th and 75th percentiles (box borders), medians (central black lines) and data ranges (whiskers). Data in **b** and **c** are presented as mean values ± s.d. of different soil carbon datasets ($n = 3$).

weathering[6]. These unique environmental conditions, combined with reduced inputs from roots, could make tropical soils more susceptible to organic matter loss under heavy grazing pressure (Fig. 3). There are also other known factors such as species composition that might help to explain the results that we did not capture in our analysis. For example, compared with C3-dominant temperate grasslands, tropical grasslands are often dominated by C4 grasses, known for their greater root density[24,25]. This characteristic has substantial influence on soil carbon dynamics in the presence of herbivory[10].

Comparison with IPCC guidelines

The IPCC guidelines typically use default carbon stock change factors to calculate grazing-driven soil carbon loss (Methods). When compared to our predicted values, we found that using IPCC's defaults results in a global underestimation of grazing-driven soil carbon loss by a factor of 3 (Fig. 4c). This discrepancy is most pronounced in the tropics, where grazing pressure is high, especially in tropical dry soils. Here our predicted losses are six times higher than those calculated using IPCC defaults (Fig. 4c). In contrast, in boreal regions, where grazing pressures are low to moderate, our estimates indicate an increase in soil carbon storage, contradicting the IPCC's suggestion of a slight decrease. These differences arise because IPCC's intensity-specific default factors do not account for the complex effects of grazing and local conditions on soil carbon changes shown in our study[16]. For example, our results suggest that heavy grazing could cause more severe soil carbon losses than expected in hotter and drier climates, while light grazing may even promote carbon storage in colder regions (Fig. 3).

Climate mitigation potential of grazing management

Overall, in line with current understanding[7], our results illustrate the complex interplay between grazing and local environmental factors in shaping soil carbon dynamics. Consistent with field observations, our global results show that soil carbon increases with GI until it reaches a

https://doi.org/10.1038/s41558-024-01957-9

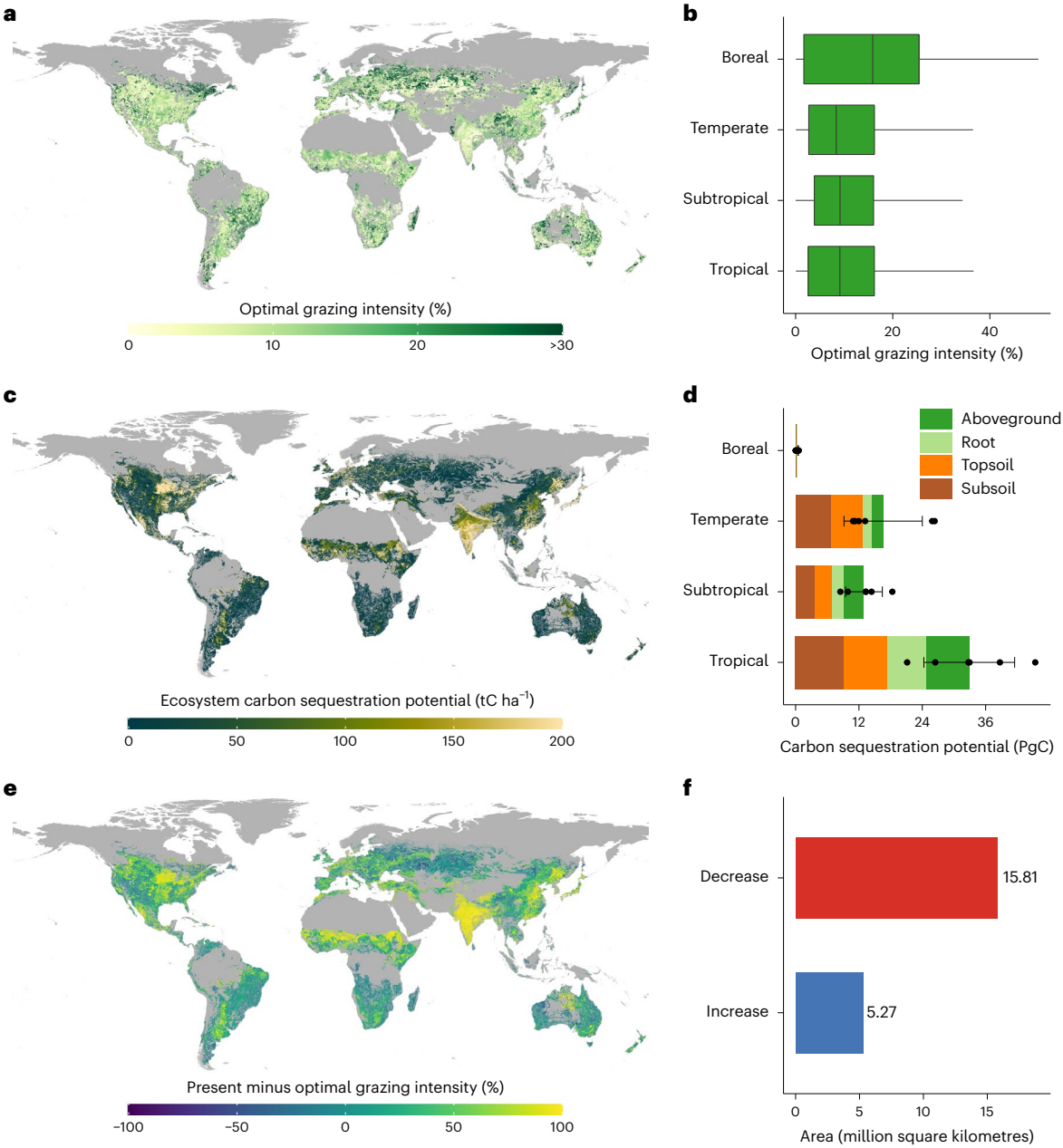

Fig. 5 | Carbon sequestration potential from grazing optimization. **a**,**b**, Global optimal grazing intensity (GI_{opt}), with the spatial pattern shown on a map (**a**) and aggregated by ecozone (**b**). **c**, Global distribution of ecosystem carbon sequestration potential (tC ha^{-1}) of grazing lands under the optimal scenario (**a**). **d**, The carbon sequestration potentials (PgC) of aboveground, root, topsoil and subsoil were aggregated by different ecozones. **e**, Differences between present-day and optimal GI. **f**, Area of grazing land where the GI needs to be increased or decreased to reach the optimal level. Box plot shows the 25th and 75th percentiles (box borders), medians (central black lines) and data ranges (whiskers). Data in **d** are shown as mean values ± s.d. for total carbon sequestration potentials across different plant and soil carbon datasets ($n = 6$).

maximum (GI_{max}) and then decreases rapidly after crossing a threshold (GI_{thres}). However, the values of GI_{max} and GI_{thres} identified are context specific and vary greatly across ecozones (Supplementary Fig. 14), depending on land use histories, as well as biotic and abiotic factors. Considering the accelerating degradation of grazing lands in many parts of the world[14], this underscores the importance of accounting for these interactions at local scales when effectively managing the fate of soil carbon to mitigate climate change.

We observed that about 4.2 million km^2 of land has exceeded the GI_{thres} due to livestock grazing (Supplementary Figs. 15 and 16), accounting for 20% of the analysed grazing lands. This threshold crossing is particularly pronounced in southern Asia, eastern North America and central Africa (Supplementary Fig. 16a), where the GI has exceeded its threshold by more than 50%. These findings underscore the need to prioritize these regions for climate change mitigation strategies. We calculated the maximum carbon sequestration potential achievable through the optimization of grazing intensity on grazing lands (Fig. 5a,b and Methods).

We found that global grazing land could sequester 63 ± 18 PgC under the optimal scenario, which offsets 12% of the historical carbon losses resulting from agricultural land uses in global vegetation biomass[26] and soils[27]. It is important to note, however, that the timing of ecosystem carbon reaching equilibrium after management implementation was not specifically addressed in this study. Since the efficiency of other nature-based solutions in carbon sequestration is often expressed as annual rates[17], a direct comparison with them

is not straightforward. We encourage future work to study carbon accrual rates in both soils and vegetation after the implementation of grazing management practices[28]. Nevertheless, by converting the carbon sequestration rates of other solutions into potentials, we found that the 63 PgC from grazing management is higher than the cumulative potential of all wetland protection pathways from 2016 to 2030 (10.5 PgC)[29]. It is comparable to the maximum biophysical scenario of 30-year natural forest regrowth, estimated at 73 PgC (ref. 30), but is almost four times lower than the recently estimated global potential for forest restoration, which stands at 226 PgC (ref. 31).

Carbon accumulation potentials from grazing optimization exhibit substantial variability worldwide, with greater values often found in eastern North America and southern Asia (Fig. 5c). Yet, despite this, we found that the tropics (33 ± 8.6 PgC) stand out as having the highest mitigation potential probably due to their larger opportunity areas (8.95 million km^2), followed by the temperate (16.6 ± 7.42 PgC; 6.89 million km^2) and subtropical (12.9 ± 3.5 PgC; 5.1 million km^2) zones (Fig. 5d and Supplementary Table 3). In addition, compared with carbon accumulated in plant (26 ± 8.1 PgC; Supplementary Table 3), around half of the mitigation potential, estimated at 37 ± 13.5 PgC, would be present in soils, where sequestered carbon can be more stable and kept for a longer period of time[17]. Nonetheless, it should be noted that this value is less than a third of the soil carbon required to offset the greenhouse gas emissions from the global ruminant sector (135 PgC)[32], indicating that relying solely on optimizing grazing is not sufficient to mitigate the warming caused by current ruminant systems.

To achieve optimal grazing intensity, our results suggest that ~75% (15.8 million km^2) of global grazing lands should be subject to reduced grazing pressures (Fig. 5e), most of which (13.7 million km^2) would need to reduce GI by at least half. The magnitude of the GI reduction is larger in middle and low latitudes (Fig. 5e). In addition, GI can be increased in about 25% (5.27 million km^2) of global grazing lands to achieve optimal GI for carbon sequestration (Fig. 5f), mainly in certain high latitudes.

Limitations

While our analysis has enabled the estimation of grazing-induced carbon changes and climate mitigation potentials with higher accuracy than previous estimates[17,33], it is important to acknowledge its limitations. First, we must emphasize that the correlations observed in our study do not necessarily imply causation (Fig. 2 and Supplementary Fig. 5). In this context, conducting field grazing experiments across multiple intensity gradients, along with detailed plot-level information (for example, plant and soil conditions), and employing specialized analytical methods (for example, structural equation modelling) could further substantiate the causal relationships, a nuance that remains a limitation in our current approach. Second, a large portion of variability in soil carbon stock change remaining unexplained (~39%). Although we have evaluated model uncertainties (Methods), it is worth noting that they reflect the bootstrap prediction uncertainty[34] and thus cannot represent other potentially important sources. The unexplained variations in soil carbon change may be attributed to limited data availability at the plot level and geographical bias in data availability (primarily from China and North America; Extended Data Fig. 1 and Supplementary Fig. 17). Often, due to the unavailability of many plot-level metadata, our model relied on interpolated global datasets with coarse spatio-temporal resolutions. Further efforts are thus required to minimize uncertainties in global datasets, primarily related to GI estimates and soil properties (Supplementary Discussion). Yet, despite these limitations, our study's comprehensive nature, encompassing a wide range of data sources and advanced analytical methods, allows us to provide a robust estimate of grazing-induced carbon changes. Our analysis, however, also brings into focus the inherent challenge of fully capturing the complex causality in ecological systems. The depth of our analysis serves to highlight the nuanced relationships within these systems, while simultaneously acknowledging the need for more targeted experiments to firmly establish causation. Last, it is important to acknowledge that our analysis did not account for the interactions between grazing and its effects on plant communities, such as above-belowground carbon allocation and species composition shifts[10], other disturbances such as fire, and future climate conditions, including global warming. These factors could potentially affect our results, particularly the estimates of the capacity of global grazing lands to capture and store carbon. Future studies should consider these interactions to provide a more comprehensive understanding of grazing land's potential in carbon sequestration.

In conclusion, our results represent both opportunities and challenges. Our work illustrates the interplay between grazing and local conditions as a major driver of soil carbon stock changes. Understanding these drivers is critical for predicting the fate of soil carbon in the future. Our analyses further suggest that global soil carbon stocks are more likely to decrease under rising temperatures and increased demand for animal products. Moreover, our high-resolution global estimates of grazing-driven soil carbon stock changes offer a robust and consistent methodology for assessing the impact of grazing on soil carbon at both global and local scales. These results also provide essential inputs for Earth system models that seek to represent grazing processes explicitly. Incorporating the grazing module into Earth system models is a challenge, but critical to improving future modelling efforts[12]. We found notable discrepancies between our predictions and the IPCC default stock change factors, especially in tropical and boreal regions. These suggest that countries using the IPCC defaults in these ecoregions may incur large errors in the grazing component of their carbon budget, underscoring a need to revise carbon stock changes due to grazing in inventory reports. Notably, since the IPCC did not account for deeper soil layers[16], we consider these differences to be conservative.

The maps of GI_{opt} and GI_{thres} should provide a data-driven roadmap for employing grazing as an effective climate mitigation solution. It will allow local governments to determine the most promising locations to develop effective policies, such as the Grassland Ecological Compensation Policy in China[35], which will help achieve a 'win–win' scenario in terms of climate mitigation and livestock production of grazing lands while also bringing other benefits such as biodiversity conservation[36]. However, achieving the potential 63 PgC sequestration under the optimal grazing scenario would require a substantial reduction in livestock production on grazing lands globally, which is particularly challenging for developing countries where large populations rely on grazing lands as their main source of income. While the specific policy-relevant livestock initiatives required to reach the optimal scenario are beyond the scope of this paper, we emphasize the need for a concerted global effort from both the supply and demand sides to make this goal feasible.

Online content

Any methods, additional references, Nature Portfolio reporting summaries, source data, extended data, supplementary information, acknowledgements, peer review information; details of author contributions and competing interests; and statements of data and code availability are available at https://doi.org/10.1038/s41558-024-01957-9.

References

1. Bradford, M. A. et al. Managing uncertainty in soil carbon feedbacks to climate change. *Nat. Clim. Change* **6**, 751–758 (2016).
2. Davidson, E. A. & Janssens, I. A. Temperature sensitivity of soil carbon decomposition and feedbacks to climate change. *Nature* **440**, 165–173 (2006).
3. Paustian, K. et al. Climate-smart soils. *Nature* **532**, 49–57 (2016).
4. Lal, R. Soil carbon sequestration impacts on global climate change and food security. *Science* **304**, 1623–1627 (2004).

5. Shi, Z. et al. The age distribution of global soil carbon inferred from radiocarbon measurements. *Nat. Geosci.* **13**, 555–559 (2020).
6. Haaf, D., Six, J. & Doetterl, S. Global patterns of geo-ecological controls on the response of soil respiration to warming. *Nat. Clim. Change* **11**, 623–627 (2021).
7. Maestre, F. T. et al. Grazing and ecosystem service delivery in global drylands. *Science* **378**, 915–920 (2022).
8. Bai, Y. F. & Cotrufo, M. F. Grassland soil carbon sequestration: current understanding, challenges, and solutions. *Science* **377**, 603–608 (2022).
9. Kristensen, J. A., Svenning, J. C., Georgiou, K. & Malhi, Y. Can large herbivores enhance ecosystem carbon persistence? *Trends Ecol. Evol.* **37**, 117–128 (2022).
10. McSherry, M. E. & Ritchie, M. E. Effects of grazing on grassland soil carbon: a global review. *Glob. Change Biol.* **19**, 1347–1357 (2013).
11. Jiang, Z. Y. et al. Light grazing facilitates carbon accumulation in subsoil in Chinese grasslands: a meta-analysis. *Glob. Change Biol.* **26**, 7186–7197 (2020).
12. Schmitz, O. J. et al. Animals and the zoogeochemistry of the carbon cycle. *Science* **362**, eaar3213 (2018).
13. Chang, J. F. et al. Climate warming from managed grasslands cancels the cooling effect of carbon sinks in sparsely grazed and natural grasslands. *Nat. Commun.* **12**, 118 (2021).
14. Bardgett, R. D. et al. Combatting global grassland degradation. *Nat. Rev. Earth Environ.* **2**, 720–735 (2021).
15. Viglizzo, E. F., Ricard, M. F., Taboada, M. A. & Vazquez-Amabile, G. Reassessing the role of grazing lands in carbon-balance estimations: meta-analysis and review. *Sci. Total Environ.* **661**, 531–542 (2019).
16. Dong, H., MacDonald, J. D., Ogle, S. M., Sanchez, M. J. S. & Rocha, M. T. *2019 Refinement to the 2006 IPCC Guidelines for National Greenhouse Gas Inventories. Volume 4: Agriculture, Forestry and Other Land Use* (IPCC, 2019).
17. Bossio, D. A. et al. The role of soil carbon in natural climate solutions. *Nat. Sustain.* **3**, 391–398 (2020).
18. Ellison, L. Influence of grazing on plant succession of rangelands. *Bot. Rev.* **26**, 1–78 (1960).
19. McNaughton, S. Grazing as an optimization process: grass–ungulate relationships in the Serengeti. *Am. Nat.* **113**, 691–703 (1979).
20. Wilson, C. H., Strickland, M. S., Hutchings, J. A., Bianchi, T. S. & Flory, S. L. Grazing enhances belowground carbon allocation, microbial biomass, and soil carbon in a subtropical grassland. *Glob. Change Biol.* **24**, 2997–3009 (2018).
21. Koerner, S. E. et al. Change in dominance determines herbivore effects on plant biodiversity. *Nat. Ecol. Evol.* **2**, 1925–1932 (2018).
22. Núñez, P., Demanet, R., Misselbrook, T., Alfaro, M. & de la Luz Mora, M. Nitrogen losses under different cattle grazing frequencies and intensities in a volcanic soil of southern Chile. *Chil. J. Agric. Res.* **70**, 237–250 (2010).
23. Zhou, G. et al. Grazing intensity significantly affects belowground carbon and nitrogen cycling in grassland ecosystems: a meta-analysis. *Glob. Change Biol.* **23**, 1167–1179 (2017).
24. Barbehenn, R. V., Chen, Z., Karowe, D. N. & Spickard, A. C3 grasses have higher nutritional quality than C4 grasses under ambient and elevated atmospheric CO_2. *Glob. Change Biol.* **10**, 1565–1575 (2004).
25. Piipponen, J. et al. Global trends in grassland carrying capacity and relative stocking density of livestock. *Glob. Change Biol.* **28**, 3902–3919 (2022).
26. Erb, K.-H. et al. Unexpectedly large impact of forest management and grazing on global vegetation biomass. *Nature* **553**, 73–76 (2018).
27. Sanderman, J., Hengl, T. & Fiske, G. J. Soil carbon debt of 12,000 years of human land use. *Proc. Natl Acad. Sci. USA* **114**, 9575–9580 (2017).
28. Sierra, C. A. et al. Carbon sequestration in the subsoil and the time required to stabilize carbon for climate change mitigation. *Glob. Change Biol.* **30**, e17153 (2024).
29. Griscom, B. W. et al. Natural climate solutions. *Proc. Natl Acad. Sci. USA* **114**, 11645–11650 (2017).
30. Cook-Patton, S. C. et al. Mapping carbon accumulation potential from global natural forest regrowth. *Nature* **585**, 545–550 (2020).
31. Mo, L. et al. Integrated global assessment of the natural forest carbon potential. *Nature* **624**, 1–10 (2023).
32. Wang, Y. et al. Risk to rely on soil carbon sequestration to offset global ruminant emissions. *Nat. Commun.* **14**, 7625 (2023).
33. Abdalla, M. et al. Critical review of the impacts of grazing intensity on soil organic carbon storage and other soil quality indicators in extensively managed grasslands. *Agric. Ecosyst. Environ.* **253**, 62–81 (2018).
34. Ma, H. et al. The global distribution and environmental drivers of aboveground versus belowground plant biomass. *Nat. Ecol. Evol.* **5**, 1110–1122 (2021).
35. Hou, L. L. et al. Grassland ecological compensation policy in China improves grassland quality and increases herders' income. *Nat. Commun.* **12**, 4683 (2021).
36. Ren, S., Cao, Y. & Li, J. Nitrogen availability constrains grassland plant diversity in response to grazing. *Sci. Total Environ.* **896**, 165273 (2023).

Methods

Data collection

We collected data on the effects of grazing on soil carbon by searching for peer-reviewed articles from the Web of Science, the China National Knowledge Infrastructure Databases and recently published meta-analysis[37], with query terms including 'grazing' and 'soil carbon' (Supplementary Fig. 18). Experiments were selected only if they met the following criteria. Grazing plots were subjected to large vertebrate herbivores (such as sheep and cattle). The study should measure at least one of soil carbon concentration, soil carbon stock or soil organic matter content at both ungrazed and grazed plots. The information on site coordinates and soil depth should be given. For enclosure studies, herbivores had to be excluded for more than 15 years, which allows soil carbon responses sufficiently to the absence of herbivores[38,39]. If studies included experiments with different grazing durations, we selected the one with the longest duration. In total, we collected 1,473 depth-specific paired observations from 294 papers published globally between 1994 and 2019.

Considering the dramatic effects of animal trampling on the physical properties of the soil (for example, bulk density)[12], here we focused on changes in carbon stocks rather than in concentration. For each study, we extracted data on mean values, standard deviations (s.d.) and sample sizes of soil carbon stock (tC ha^{-1}; $n = 540$ pairs) from tables or figures using the GetData (v.2.25) software. Furthermore, we recorded data on site coordinates, climate, elevation, vegetation types, above- and belowground plant biomass ($n = 859$ and 543, respectively), soil depth (ranging from upper 5 cm to longer than 1 m), bulk density (g cm^{-3}; $n = 558$), soil carbon concentration (g kg^{-1}; $n = 948$), soil organic matter (g kg^{-1}; $n = 275$), C:N ratio ($n = 342$), clay content (%; $n = 119$), grazing intensity categories (light, moderate and heavy; $n = 1{,}111$), livestock species (single and mixed; $n = 955$), grazing duration ($n = 715$; ranging from less than 1 year to 60 years). In addition, we classified soil samples into tropical, subtropical, temperate and boreal ecozones based on site-specific coordinates and Food and Agriculture Organization ecozones[40].

About 37% ($n = 540$ of 1,473) measurements provided soil carbon stock data. For the remaining data, soil carbon stocks were converted from soil organic matter ($n = 191$) or soil carbon concentration ($n = 742$). When experiments only measured soil organic matter, we estimated soil carbon concentration as soil organic matter content/2 (ref. 41). Soil carbon concentration data were converted to stocks based on soil bulk density and soil depth. Specially, when data on bulk density were not provided ($n = 625$), we estimated them based on empirical relationships between soil carbon concentration (SOC; g kg^{-1}) and bulk density (BD; g cm^{-3}) across the reported data for control and grazed sites (equations (1) and (2) and Supplementary Fig. 19).

$$BD_{control} = 1.25 \times e^{-0.013SOC} + 0.25, R^2 = 0.63, P < 0.001 \quad (1)$$

$$BD_{grazed} = 1.23 \times e^{-0.012SOC} + 0.25, R^2 = 0.53, P < 0.001 \quad (2)$$

In our compiled dataset, about 75% ($n = 1{,}111$ of 1,473) measurements provided clear information on grazing intensity category (that is light, moderate and heavy intensity). Most studies used the proportion of aboveground biomass consumed as an indicator of grazing intensity[13,42]. We analysed the changes in aboveground plant biomass at different grazing intensity categories with reported values (Supplementary Fig. 20). For studies that only provided data on GI categories or aboveground plant biomass, we defined light, moderate and heavy grazing intensities as 0–30%, 30–50% and >50% reduction in biomass, respectively, which is consistent with previous studies[13]. Specially, for a few mearsurements where aboveground plant biomass increases ($n = 9$), we defined them as moderate grazing intensity according to grazing optimization hypothesis[18,19].

Meta-analysis

We calculated the natural logarithm of the response ratio (LRR) as a metric to quantify the effect of grazing on soil carbon stocks for each experiment. Effect sizes were calculated using the escalc function from the metafor package in R (ref. 43).

$$LRR = \ln\left(\frac{X_G}{X_C}\right) = \ln(X_G) - \ln(X_C) \quad (3)$$

with X_C and X_G as mean values of the variables in the control and grazed treatments, respectively. We also obtained the variances of LRR to calculate overall effects and 95% CI using rma.mv function in metafor, in which the variable 'site' was included as a random factor and effect sizes from individual experiments were weighted by the inverse of the variance. The bias-corrected 95% bootstrapped CIs in this study were estimated using the Wald-type method, which is based on the assumption of a normal distribution for the underlying data[43]. The effect of grazing is considered significant if the 95% CI does not overlap zero. If standard error was reported instead of s.d. in a study, s.d. was calculated from standard error. For experiments that did not provide SD or standard error ($n = 236$ of 1,473), Rubin and Schenker's resampling approach from the R package metagear was employed[44]. This approach enables the estimation of s.d. even when only mean values are available in a study through resampling from experiments with similar means[44,45]. The percentage change in soil carbon stocks was derived by the back-transformation of the response ratio ($e^{(\ln R \cdot 1)} \times 100$).

We performed Egger's regression and fail-safe analysis to test for publication bias. Specially, we used regtest function in R metafor package to test for bias[46], and found that P value for the test is less than 0.05 for most categorical variables (Supplementary Table 4), indicating that publication bias exits. To further investigate the potential impact of unpublished articles on our results, we performed the Rosenberg fail-safe number analysis (fsn function)[47]. It is considered likely that unpublished articles have an effect when the Rosenberg fail-safe number is less than $5N + 10$ (N represents the number of observations). In our case, the Rosenberg fail-safe numbers were greater than $5N + 10$ (Supplementary Table 4).

Identifying important variables

To identify the important predictors of the grazing effect on carbon stocks across grazing experiments, we selected ten uncorrelated variables, including climate (mean annual temperature and mean annual precipitation), vegetation (normalized difference vegetation index), soil (depth, organic carbon content, C:N ratio and clay content), anthropogenic (grazing intensity) and experimental (duration and livestock types) features. Using the R package randomForest[48], we ran a random forest model to quantify the relative importance of these factors of soil carbon change across the globe (Fig. 4). This approach is robust in dealing with multiple predictors and their interactions as well as considering non-linear relationships[45].

Upscaling grazing-driven soil carbon stock changes across the globe

Acquisition of environmental covariates. To create a spatially predictive model of the effect of grazing on soil carbon stocks, we first sampled our prepared stack of 84 environmental covariates at each independent data point within the compiled grazing database. These layers included atmospheric, climatic, soil depth, soil nutrient, soil physical, soil chemical, vegetation, topography and anthropogenic variables (Supplementary Table 5), which have notable effects on soil carbon change (Fig. 1). Specially, values from all gridded environmental layers were extracted based on site-specific coordinate information, while soil depth and grazing intensity information were taken from original studies.

Geospatial modelling. To minimize the influence of 'extreme' values, we identified outliers as the values exceeding −3 or +3 s.d. from the population mean. Consequently, three data were removed in our

analysis. We used the R packages metaforest[49] and caret[50] to train a global model on 84 environmental covariates across data points (n = 1,329). The approach is based on the machine-learning 'random forest' algorithm[49] that can handle many types of predictors as well as their interactions, and is integrated in a meta-analytic context by including the variances and weights of each experiment[45]. We used a grid-search procedure, with tenfold cross-validation, to select the best hypermeter combination for the meta-forest model with the lowest cross-validation root mean square error (RMSE) (R^2 = 0.61, RMSE 0.22; Supplementary Fig. 9). To test for and quantify the potential effect of spatial autocorrelation in the model residuals, we performed Moran *I* test[51] and found the Moran *I* statistic is −0.052 (P > 0.05), indicating a non-significant spatial autocorrelation in our data. We then used the best meta-forest model to predict global high-resolution (~1 km) maps of grazing-driven soil carbon change at each vertical increment of 5 cm to a soil depth of 1 m, which were further aggregated into two maps for topsoil (0–30 cm) and subsoil (30–100 cm). All covariate maps (except GI, which was calculated; see below) were resampled and reprojected to a unified pixel grid in EPSG:4326 (WGS84) at 30-arcsecond resolution (~1 km at the Equator).

The absolute changes in soil carbon stocks and associated uncertainties were calculated on the basis of three present-day datasets of soil carbon stocks (equations (4) and (5)).

$$\Delta SCS_{abs} = (SCS - \Delta SCS_{abs}) \times \frac{\Delta SCS_{rel}}{100} \quad (4)$$

Using the equation, we can derive

$$\Delta SCS_{abs} = \frac{SCS \times \Delta SCS_{rel}/100}{(1 + \Delta SCS_{rel}/100)} \quad (5)$$

where ΔSCS_{abs} and ΔSCS_{rel} represent the absolute (tC ha^{-1}) and relative (%) changes of soil carbon stocks after grazing, respectively. SCS is present-day soil carbon stocks derived from SoilGrids 2.0 (ref. 52), Harmonized World Soil Database (HWSD)[53] and the Global Soil Dataset for Earth System Modeling (GSDE)[54] datasets. In addition, soil carbon storge changes in units of PgC were calculated by multiplying ΔSCS_{abs} by grazing area.

Deriving grazing intensity at a global scale. Here we used the ratio of grazed biomass to aboveground net primary production (ANPP) available for grazing as an indicator of grazing intensity (equation (6)). This metric, which was widely used in previous studies[13,42,55–57], has the advantage in introducing an unambiguous baseline that is purely dependent on natural conditions, and allows to provide a meaningful and comparable measure for grazing pressures among different ecosystems[42].

$$\text{Grazing intensity} = \frac{TLU \times FI}{GA \times ANPP} \times 100 \quad (6)$$

where TLU refers to tropical livestock units (one TLU equals 250 kg live weight)[58] and GA is grazing area per grid cell. FI represents grass feed intake, defined as the amount of biomass consumed per TLU per year. In this study, we derived FI data from Fetzel et al.[42], which are available at a regional level and have accounted for diverse factors (for example, the feed structure for different livestock types, livestock in different livestock production systems)[55,59–61]. Noting that here we focused only on forage from grazing land, excluding feedstuff from other sources[42]. By employing livestock units, we can easily compare diverse types of livestock and effectively estimate grid-level FI by leveraging gridded livestock data (see below).

It is straightforward that the uncertainty in GI estimates stems from the different global datasets and their own uncertainties. In this study, we used Monte Carlo approach to bring combined uncertainties of datasets into GI estimates. First, in contrast to previous studies, ANPP was estimated directly by difference between NPP and belowground net primary production (BNPP). Specifically, two present-day NPP datasets (MODIS[62] and GIMMS3g[63]) were used. For both NPP dataset, we assumed the values might vary 7% in each grid cell[25]. Global BNPP was derived from a recent study[64], which mapped the global distribution of BNPP and its uncertainty at 1-km resolution based on filed observations. Two global maps of the extent of grazing land and their uncertainties were used in this study[65,66]. Moreover, the gridded map of TLU was calculated based on information on TLU numbers per head for livestock species[58] and the global patterns of cattle, buffaloes, sheep, goats and horse from the Gridded Livestock of the World database[67]. Here we assumed the value of the livestock database might vary 10% in each grid cell. For each dataset, we assumed truncated normal distributions and randomly created 100 samples within the uncertainty range. Finally, these 400 GI estimates (100 samples × 2 NPP datasets × 2 grazing extent maps) were used to calculate the mean and s.d. (Supplementary Fig. 11).

Notably, due to the accumulation of uncertainties arising from various input datasets (Supplementary Discussion), approximately 5% of the grazing area exhibits GI values exceeding 100%, mainly in southern Asia and central Africa. Previous studies have suggested that these regions are indeed experiencing severe overgrazing[13,25,68]. Therefore, in this study, we assigned a heavy grazing intensity to these areas and have varified that this adjustment did not alter our conclusions (Supplementary Fig. 21).

Uncertainty and extent of extrapolation. To create per-pixel CIs in estimations of soil carbon change, we performed a bootstrapping procedure in R v4.0.5 software. In this analysis, the training dataset is resampled 100 times with replacement. We then used these bootstrapped resamples to train 100 meta-forest models and calculated coefficient of variation on the basis of these 100 models' predictions for each pixel at each vertical increment of 5 cm to a soil depth of 1 m (Supplementary Fig. 22). We also assessed the extent of extrapolation in our models by examining how well training data represents the univariate environmental covariate space[69]. We first determined the sample range through deriving the minimum and maximum values for each of the 84 global covariate layers. Then we evaluated the number of variables that fell inside and outside the sample ranges for each pixel and created a final image that represents the proportion of bands where the pixel value falls within the sample range (Supplementary Fig. 17). About 97% of predicted pixels with values fell within the sample range of at least 90% of all bands. The average percentage of pixels with values within the sample range of the covariate layers was 98%. It is worth noting that although our sample covers most of the environmental conditions on Earth, there are some regions (e.g., some tropics and high latitudes; 25% of grazing area) that are not well represented in our grazing experiments (Extended Data Fig. 1 and Supplementary Fig. 17), and we therefore excluded these regions from our analysis.

Nonlinear responses of soil carbon change to GI. We also examined the non-linear relationships between soil carbon change and GI for each ecozone using our global estimates (Supplementary Fig. 14). We selected general additive models (package mgcv[70]), which is good at the modelling of complex relationships between variables, to describe the complexity of non-linear trends between soil carbon change and GI. Only when non-linear regressions were a better fit to the relationship between GI and soil carbon change, threshold in GI may be present for each ecozone[70]. We here defined the threshold as the point after the GI_{max} where carbon stocks start to decrease sharply with increasing GI. Using the package 'segmented'[71] in R, we explored the threshold on the basis of segmented regression, which detected the abrupt changes in the slope on both sides of the threshold.

Comparison of predicted values with the IPCC defaults. To compare our predicted grazing-driven soil carbon changes to those calculated using the IPCC default stock change factors, we first summarized our predictions using the IPCC climate zones. Then, we calculated soil carbon storage change (ΔSC) using the IPCC default factors at a level of climate zone (equation (7)).

$$\Delta SC = SCS_{ref} \times (F_{MG} - 1) \times GA \quad (7)$$

where SCS_{ref} and F_{MG} represent reference soil carbon stock (tC ha^{-1}) and grazing management factor, respectively, derived from the IPCC[16]. Specially, F_{MG} is 1 for light grazing and 0.7 for heavy grazing category. For moderate grazing, F_{MG} is 0.97 for tropical regions and 0.95 for the rest of the world. GA is the grazing area for each climate zone. Notably, since the IPCC's default factors are only available at a depth of 30 cm, we focus here on carbon storage change in this soil layer.

Deriving root biomass carbon change at a global scale

To evaluate the effects of grazing on root carbon storage, we also collected 738 paired observations and generated a global distribution of root biomass carbon change and its uncertainty (Supplementary Figs. 12 and 13), using the same approach as for soil carbon (see above). The predictive model was trained on atmospheric, climatic and anthropogenic variables and showed a good performance (tenfold cross-validated R^2 = 0.84, RMSE 0.24; Supplementary Fig. 12). The absolute changes in biomass carbon density and associated uncertainties were calculated on the basis of two present-day biomass datasets of harmonized global above and belowground biomass carbon density maps[72] and the IPCC Tier-1 maps[73]. We also evaluated variable importance for root carbon change across filed experiments and found that grazing intensity was the most important factor controlling the responses of root carbon to grazing (Supplementary Fig. 4).

Mapping optimal grazing intensity at a global scale

To assess the climate mitigation potential through grazing optimization, we explored the optimal grazing intensity (GI_{opt}) at a global scale. To do this, we employed a moving-window approach and established predictive models that incorporated grazing and local environmental factors within each window (Supplementary Fig. 23). By doing so, we determined GI_{opt} that can achieve maximum carbon storage (Fig. 5a) and GI_{thres} at which carbon stocks start to decline rapidly at the grid level (Supplementary Fig. 15).

Specifically, to account for the interactions between grazing and local environmental factors, we trained predictive models (random forest[48] and general additive model[70]) for the relative changes (LRR) in three belowground carbon components (root, topsoil and subsoil) on 12 important variables (including grazing intensity, mean annual temperature, mean annual precipitation, aridity, normalized difference vegetation index, species richness[74], elevation, soil pH, soil carbon content, soil nitrogen content, soil C:N ratio and soil clay content) within a pre-defined buffer zone radius from the examined point (Supplementary Fig. 23). The identified radius had to meet the following criteria: (1) within the buffer zone, data points should be distributed over at least eight gradients of grazing intensity (from 0% to 80% with 10% interval); (2) to reduce the confounding effects of environmental heterogeneity, the radius should be as small as possible; and (3) to ensure consistency, the radius should be as uniform as possible among pixels. Following these guidelines, for each grid cell, we started with 0 km and searched for the desired radius in increments of 5 km (Δr_5) and 10 km (Δr_{10}).

For each analysed grid, we entered its environmental conditions into the predictive models, predicted the three belowground carbon component changes with GI ranging from 0% to 80%, and then converted them to absolute terms. Specially, global biomass datasets were from harmonized global above and belowground biomass carbon density maps[72] and the IPCC Tier-1 maps[73], and soil carbon datasets were from SoilGrids 2.0 (ref. 52), HWSD[53] and GSDE[54]. To account for livestock production and carbon sequestration potential trade-offs, we focused on the absolute changes in belowground carbon stocks (ΔBCS) and extracted the grazing intensity (GI_{max}) where the ΔBCS was maximum (ΔBCS_{max}). In addition, we derived GI_{thres} that lead to abrupt decay in ΔBCS for each grid cell using the same approach detailed above. Noting that GI_{thres} should be larger than GI_{max}. To better constrain GI_{opt}, we compared the changes in ecosystem carbon stocks (ΔECS) at GI_{max} (ΔECS_{max}) to that (ΔECS_{pres}) at the present-day grazing intensity (GI_{pres}). Here, we focused on ΔECS rather than ΔBCS in order to derive more explicit and reasonable GI_{opt}. For example, if ΔBCS_{max} is higher than the present-day ΔBCS, but this is reversed for aboveground carbon (that is, $GI_{max} < GI_{pres}$), then it would be difficult to determine that GI_{max} is the optimal. If $\Delta ECS_{max} > \Delta ECS_{pres}$, $GI_{opt} = GI_{max}$; (2) $\Delta ECS_{max} < \Delta ECS_{pres}$, GI_{opt} is not determined; (3) $\Delta ECS_{max} = \Delta ECS_{pres}$, $GI_{opt} = \max\{GI_{max}, GI_{pres}\}$. Under optimal scenarios, the carbon sequestration potential of grazing lands was calculated by the difference between ΔECS_{max} and ΔECS_{pres}.

We used the Monte Carlo approach to account for uncertainties in our estimates. Specially, for each grid cell, we developed ten predictive models by randomly generating samples for each of four carbon components. Combined with different Δr values, predictive models and data sources of carbon stocks, s.d. were then derived from 240 ensemble members (10 × 2 Δr × 2 predictive model types × 2 biomass carbon datasets × 3 soil carbon datasets) (Supplementary Fig. 24).

Reporting summary

Further information on research design is available in the Nature Portfolio Reporting Summary linked to this article.

Data availability

The two grazing fraction maps used in this study can be obtained from https://boku.ac.at/wiso/sec/data-download and http://www.earthstat.org/cropland-pasture-area-2000/, respectively. The soil carbon stock datasets of SoilGrids 2.0, HWSD and the GSDE are available at https://soilgrids.org/, http://www.fao.org/soils-portal/data-hub/soil-maps-and-databases/harmonized-world-soil-database-v12/en/ and http://www.fao.org/soils-portal/data-hub/soil-maps-and-databases/harmonized-world-soil-database-v12/en/, respectively. The plant biomass maps of harmonized global above and belowground biomass carbon density and the IPCC Tier-1 are available at https://doi.org/10.3334/ORNLDAAC/1763 and https://doi.org/10.15485/1463800, respectively. The collected metadata and maps have been deposited in the Figshare data repository (https://doi.org/10.6084/m9.figshare.21972521)[75].

Code availability

All data analysis and plotting (including global maps) for this study were performed or created using R v.4.0.5. The code is available at the Figshare data repository (https://doi.org/10.6084/m9.figshare.21972521)[75].

References

37. Lai, L. M. & Kumar, S. A global meta-analysis of livestock grazing impacts on soil properties. *PLoS ONE* **15**, e0236638 (2020).
38. Xiong, D. P., Shi, P. L., Zhang, X. Z. & Zou, C. B. Effects of grazing exclusion on carbon sequestration and plant diversity in grasslands of China—a meta-analysis. *Ecol. Eng.* **94**, 647–655 (2016).
39. Hu, Z. M. et al. A synthesis of the effect of grazing exclusion on carbon dynamics in grasslands in China. *Glob. Change Biol.* **22**, 1385–1393 (2016).
40. *Global Ecological Zoning for the Global Forest Resources Assessment, 2000* (FAO, 2001).
41. Pribyl, D. W. A critical review of the conventional SOC to SOM conversion factor. *Geoderma* **156**, 75–83 (2010).

42. Fetzel, T. et al. Quantification of uncertainties in global grazing systems assessment. *Glob. Biogeochem. Cycles* **31**, 1089–1102 (2017).
43. Viechtbauer, W. Conducting meta-analyses in R with the metafor package. *J. Stat. Softw.* **36**, 1–48 (2010).
44. Lajeunesse, M. J. Facilitating systematic reviews, data extraction and meta-analysis with the metagear package for R. *Methods Ecol. Evol.* **7**, 323–330 (2016).
45. Terrer, C. et al. A trade-off between plant and soil carbon storage under elevated CO_2. *Nature* **591**, 599–603 (2021).
46. Sterne, J. A. C., Gavaghan, D. & Egger, M. Publication and related bias in meta-analysis: power of statistical tests and prevalence in the literature. *J. Clin. Epidemiol.* **53**, 1119–1129 (2000).
47. Rosenberg, M. S. The file-drawer problem revisited: a general weighted method for calculating fail-safe numbers in meta-analysis. *Evolution* **59**, 464–468 (2005).
48. Liaw, A. & Wiener, M. Classification and regression by randomForest. *R. N.* **2**, 18–22 (2002).
49. Van Lissa, C. J. MetaForest: exploring heterogeneity in meta-analysis using random forests. Preprint at https://psyarxiv.com/myg6s/ (2017).
50. Kuhn, M. Building predictive models in R using the caret package. *J. Stat. Softw.* **28**, 1–26 (2008).
51. Moran, P. A. A test for the serial independence of residuals. *Biometrika* **37**, 178–181 (1950).
52. Hengl, T. et al. SoilGrids250m: global gridded soil information based on machine learning. *PLoS ONE* **12**, e0169748 (2017).
53. Wieder, W., Boehnert, J., Bonan, G. & Langseth, M. *Regridded Harmonized World Soil Database v1. 2* (ORNL DAAC, 2014).
54. Shangguan, W., Dai, Y., Duan, Q., Liu, B. & Yuan, H. A global soil data set for Earth system modeling. *J. Adv. Model. Earth Syst.* **6**, 249–263 (2014).
55. Bouwman, A. F., Van der Hoek, K. W., Eickhout, B. & Soenario, I. Exploring changes in world ruminant production systems. *Agric. Syst.* **84**, 121–153 (2005).
56. Haberl, H. et al. Quantifying and mapping the human appropriation of net primary production in Earth's terrestrial ecosystems. *Proc. Natl Acad. Sci. USA* **104**, 12942–12945 (2007).
57. Petz, K. et al. Mapping and modelling trade-offs and synergies between grazing intensity and ecosystem services in rangelands using global-scale datasets and models. *Glob. Environ. Change* **29**, 223–234 (2014).
58. Rothman-Ostrow, P., Gilbert, W. & Rushton, J. Tropical livestock units: re-evaluating a methodology. *Front. Vet. Sci.* **7**, 556788 (2020).
59. Herrero, M. et al. Biomass use, production, feed efficiencies, and greenhouse gas emissions from global livestock systems. *Proc. Natl Acad. Sci. USA* **110**, 20888–20893 (2013).
60. Robinson, T. P. et al. *Global Livestock Production Systems* (FAO and ILRI, 2011).
61. Krausmann, F. et al. Global human appropriation of net primary production doubled in the 20th century. *Proc. Natl Acad. Sci. USA* **110**, 10324–10329 (2013).
62. Zhao, M. S. & Running, S. W. Drought-induced reduction in global terrestrial net primary production from 2000 through 2009. *Science* **329**, 940–943 (2010).
63. Smith, W. K. et al. Large divergence of satellite and Earth system model estimates of global terrestrial CO_2 fertilization. *Nat. Clim. Change* **6**, 306–310 (2016).
64. Xiao, L. J. et al. Global depth distribution of belowground net primary productivity and its drivers. *Glob. Ecol. Biogeogr.* **32**, 1435–1451 (2023).
65. Erb, K.-H. et al. A comprehensive global 5 min resolution land-use data set for the year 2000 consistent with national census data. *J. Land Use Sci.* **2**, 191–224 (2007).
66. Ramankutty, N., Evan, A. T., Monfreda, C. & Foley, J. A. Farming the planet: 1. Geographic distribution of global agricultural lands in the year 2000. *Glob. Biogeochem. Cycles* **22**, GB1003 (2008).
67. Gilbert, M. et al. Global distribution data for cattle, buffaloes, horses, sheep, goats, pigs, chickens and ducks in 2010. *Sci. Data* **5**, 180227 (2018).
68. Oldeman, L., Hakkeling, R., Sombroek, W. & Batjes, N. *Global Assessment of Human-Induced Soil Degradation (GLASOD)* (ISRIC World Soil Information, 1991).
69. van den Hoogen, J. et al. Soil nematode abundance and functional group composition at a global scale. *Nature* **572**, 194–198 (2019).
70. Berdugo, M. et al. Global ecosystem thresholds driven by aridity. *Science* **367**, 787–790 (2020).
71. Muggeo, V. M. Segmented: an R package to fit regression models with broken-line relationships. *R. N.* **8**, 20–25 (2008).
72. Spawn, S. A., Sullivan, C. C., Lark, T. J. & Gibbs, H. K. Harmonized global maps of above and belowground biomass carbon density in the year 2010. *Sci. Data* **7**, 112 (2020).
73. Gibbs, H. K. & Ruesch, A. *New IPCC Tier-1 Global Biomass Carbon Map for the Year 2000* (Carbon Dioxide Information Analysis Center, Oak Ridge National Laboratory, 2008).
74. Cai, L. et al. Global models and predictions of plant diversity based on advanced machine learning techniques. *N. Phytol.* **237**, 1432–1445 (2023).
75. Ren, S. et al. Data and code for 'Historical impacts of grazing on carbon stocks and climate mitigation opportunities'. *Figshare* https://doi.org/10.6084/m9.figshare.21972521 (2024).

Acknowledgements

We sincerely appreciate all the scientists who contribute their precious data for our synthesis study. We thank Z. Luo for providing global BNPP and its uncertainty datasets. This work was supported by the Second Tibetan Plateau Scientific Expedition and Research Program (2019QZKK0606 and 2022QZKK0101) and Science and Technology Major Project of Tibetan Autonomous Region of China (XZ202201ZD0005G01). C.T. acknowledges support from the MIT Climate and Sustainability Consortium (MCSC).

Author contributions

S.R. conceived the idea for the study, and developed the concept together with C.T. and D.L. S.R. performed the data analysis and wrote the manuscript, with major contributions provided by C.T. All the authors contributed to the discussions and paper revision.

Competing interests

The authors declare no competing interests.

Additional information

Extended data is available for this paper at https://doi.org/10.1038/s41558-024-01957-9.

Supplementary information The online version contains supplementary material available at https://doi.org/10.1038/s41558-024-01957-9.

Correspondence and requests for materials should be addressed to Shuai Ren, César Terrer or Dan Liu.

Peer review information *Nature Climate Change* thanks Liming Lai, Shawn Leroux and the other, anonymous, reviewer(s) for their contribution to the peer review of this work.

https://doi.org/10.1038/s41558-024-01957-9

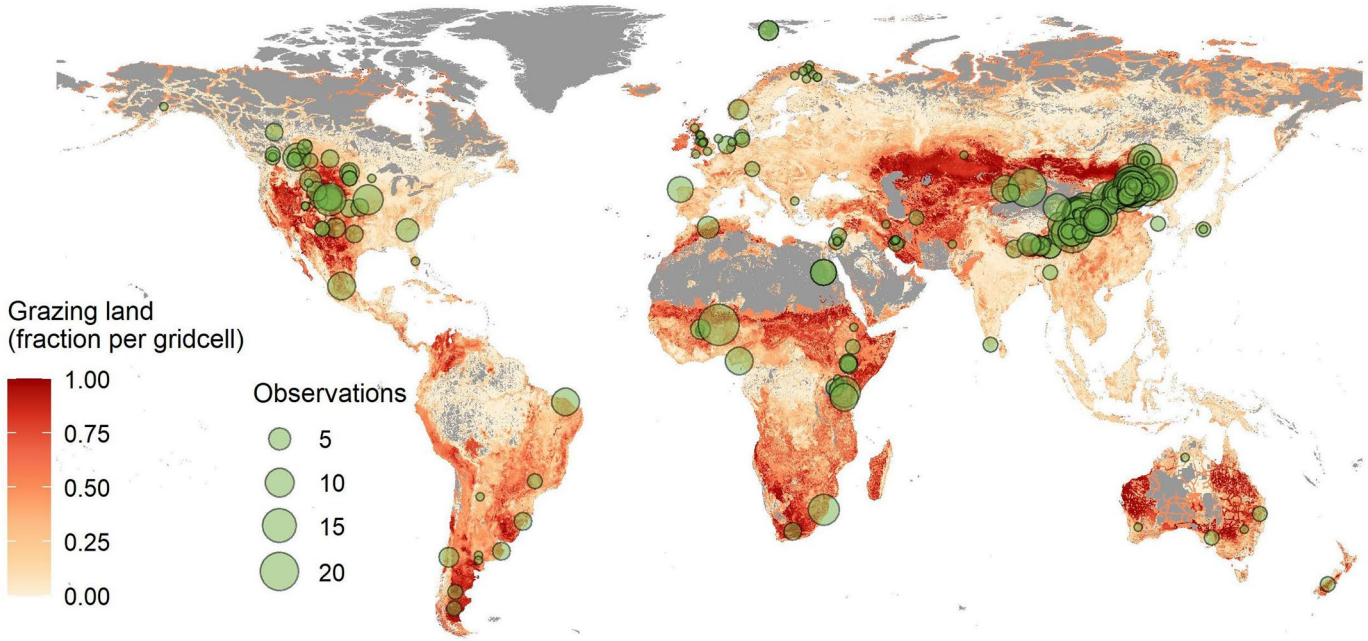

Extended Data Fig. 1 | Location of 1,473 soil samples. Sites are overlaid on the global map of grazing fraction, which is derived from Erb et al.[65] and Ramankutty et al.[66].

nature portfolio

Corresponding author(s): Shuai Ren, César Terrer, Dan Liu

Last updated by author(s): Feb 15, 2024

Reporting Summary

Nature Portfolio wishes to improve the reproducibility of the work that we publish. This form provides structure for consistency and transparency in reporting. For further information on Nature Portfolio policies, see our Editorial Policies and the Editorial Policy Checklist.

Statistics

For all statistical analyses, confirm that the following items are present in the figure legend, table legend, main text, or Methods section.

n/a	Confirmed	
☐	☒	The exact sample size (*n*) for each experimental group/condition, given as a discrete number and unit of measurement
☐	☒	A statement on whether measurements were taken from distinct samples or whether the same sample was measured repeatedly
☐	☒	The statistical test(s) used AND whether they are one- or two-sided *Only common tests should be described solely by name; describe more complex techniques in the Methods section.*
☐	☒	A description of all covariates tested
☐	☒	A description of any assumptions or corrections, such as tests of normality and adjustment for multiple comparisons
☐	☒	A full description of the statistical parameters including central tendency (e.g. means) or other basic estimates (e.g. regression coefficient) AND variation (e.g. standard deviation) or associated estimates of uncertainty (e.g. confidence intervals)
☐	☒	For null hypothesis testing, the test statistic (e.g. *F*, *t*, *r*) with confidence intervals, effect sizes, degrees of freedom and *P* value noted *Give P values as exact values whenever suitable.*
☒	☐	For Bayesian analysis, information on the choice of priors and Markov chain Monte Carlo settings
☒	☐	For hierarchical and complex designs, identification of the appropriate level for tests and full reporting of outcomes
☒	☐	Estimates of effect sizes (e.g. Cohen's *d*, Pearson's *r*), indicating how they were calculated

Our web collection on statistics for biologists contains articles on many of the points above.

Software and code

Policy information about availability of computer code

Data collection	Data was collected manually from peer-reviewed publications using GetData (v.2.25) software. Details were reported in Methods.
Data analysis	All analyses were performed in R v4.0.5. The R packages used in this study include metafor, metagear, randomForest, metaforest, caret, mgcv. The code are available at https://figshare.com/s/d9290860dd63dbcdd8b9

For manuscripts utilizing custom algorithms or software that are central to the research but not yet described in published literature, software must be made available to editors and reviewers. We strongly encourage code deposition in a community repository (e.g. GitHub). See the Nature Portfolio guidelines for submitting code & software for further information.

Data

Policy information about availability of data

All manuscripts must include a data availability statement. This statement should provide the following information, where applicable:

- Accession codes, unique identifiers, or web links for publicly available datasets
- A description of any restrictions on data availability
- For clinical datasets or third party data, please ensure that the statement adheres to our policy

The two grazing fraction datasets can be obtained from https://boku.ac.at/wiso/sec/data-download and http://www.earthstat.org/cropland-pasture-area-2000/, respectively. The soil carbon stock datasets of SoilGrids 2.0, Harmonized World Soil Database and the Global Soil Dataset for Earth System Modeling are available at https://soilgrids.org/, http://www.fao.org/soils-portal/data-hub/soil-maps-and-databases/harmonized-world-soil-database-v12/en/ and http://www.fao.org/soils-

portal/data-hub/soil-maps-and-databases/harmonized-world-soil-database-v12/en/, respectively. The plant biomass datasets of harmonized global above and belowground biomass carbon density maps and the IPCC Tier-1 maps are available at https://doi.org/10.3334/ORNLDAAC/1763 and https://doi.org/10.15485/1463800, respectively. The collected metadata and maps have been deposited in the Figshare data repository (https://figshare.com/s/d9290860dd63dbcdd8b9).

Human research participants

Policy information about studies involving human research participants and Sex and Gender in Research.

Reporting on sex and gender	n/a
Population characteristics	n/a
Recruitment	n/a
Ethics oversight	n/a

Note that full information on the approval of the study protocol must also be provided in the manuscript.

Field-specific reporting

Please select the one below that is the best fit for your research. If you are not sure, read the appropriate sections before making your selection.

☐ Life sciences ☐ Behavioural & social sciences ☒ Ecological, evolutionary & environmental sciences

For a reference copy of the document with all sections, see nature.com/documents/nr-reporting-summary-flat.pdf

Ecological, evolutionary & environmental sciences study design

All studies must disclose on these points even when the disclosure is negative.

Study description	We used a global dataset of soil carbon stocks from 1,473 grazing experiments, combined with 84 global layers of climate, vegetation, soil and anthropogenic features, to train a machine learning model for generating global high-resolution maps of grazing-driven carbon stock changes for different soil layers. We additionally explored the controls of the trends in grazing effects across the globe and within each ecozone and estimated carbon sequestration potential of grazing lands through grazing optimization.
Research sample	Plot-level soil carbon responses to grazing.
Sampling strategy	No statistical methods were used to predetermine sample size.
Data collection	Data was collected through literature search.
Timing and spatial scale	Soil carbon data from all continents except Antarctica, collected after the year 1994 were used in this study.
Data exclusions	Experiments were only selected if they met the following criteria. (1) Grazing plots were subjected to large vertebrate herbivores (such as sheep, cattle). (2) The study should measure at least one of soil carbon concentration, soil carbon density or soil organic matter at both ungrazed and grazed plots. (3) The information on site coordinates and soil depth should be given. (4) For enclosure studies, herbivores had to be excluded for more than 15 years, which allows soil carbon responses sufficiently to the absence of herbivores. If studies included experiments with different grazing durations, we selected the one with the longest duration.
Reproducibility	n/a
Randomization	n/a
Blinding	n/a

Did the study involve field work? ☐ Yes ☒ No

Reporting for specific materials, systems and methods

We require information from authors about some types of materials, experimental systems and methods used in many studies. Here, indicate whether each material, system or method listed is relevant to your study. If you are not sure if a list item applies to your research, read the appropriate section before selecting a response.

Materials & experimental systems

n/a	Involved in the study
☒	☐ Antibodies
☒	☐ Eukaryotic cell lines
☒	☐ Palaeontology and archaeology
☒	☐ Animals and other organisms
☒	☐ Clinical data
☒	☐ Dual use research of concern

Methods

n/a	Involved in the study
☒	☐ ChIP-seq
☒	☐ Flow cytometry
☒	☐ MRI-based neuroimaging